Stem Cell Reports
Report

ISSCR

OPEN ACCESS

Efficient Large-Scale 2D Culture System for Human Induced Pluripotent Stem Cells and Differentiated Cardiomyocytes

Shugo Tohyama,[1,2] Jun Fujita,[1,*] Chihana Fujita,[1] Miho Yamaguchi,[1] Sayaka Kanaami,[1] Rei Ohno,[1] Kazuho Sakamoto,[4,6] Masami Kodama,[5] Junko Kurokawa,[6] Hideaki Kanazawa,[1] Tomohisa Seki,[1] Yoshikazu Kishino,[1] Marina Okada,[1] Kazuaki Nakajima,[1] Sho Tanosaki,[1] Shota Someya,[1] Akinori Hirano,[3] Shinji Kawaguchi,[3] Eiji Kobayashi,[2] and Keiichi Fukuda[1]

[1]Department of Cardiology, Keio University School of Medicine, 35 Shinanomachi, Shinjuku-ku, Tokyo 160-8582, Japan
[2]Department of Organ Fabrication, Keio University School of Medicine, 35 Shinanomachi, Shinjuku-ku, Tokyo 160-8582, Japan
[3]Department of Cardiovascular Surgery, Keio University School of Medicine, 35 Shinanomachi, Shinjuku-ku, Tokyo 160-8582, Japan
[4]Department of Pharmacology, Fukushima Medical University School of Medicine, 1 Hikarigaoka, Fukushima 960-1295, Japan
[5]Department of Bio-informational Pharmacology, Medical Research Institute, National University Corporation Tokyo Medical and Dental University, 1-5-45 Yushima, Bunkyo-ku, Tokyo 113-8510, Japan
[6]Department of Bio-Informational Pharmacology, School of Pharmaceutical Sciences, University of Shizuoka, 52-1 Yada, Suruga-ku, Shizuoka 422-8526, Japan
*Correspondence: jfujita@a6.keio.jp
http://dx.doi.org/10.1016/j.stemcr.2017.08.025

SUMMARY

Cardiac regenerative therapies utilizing human induced pluripotent stem cells (hiPSCs) are hampered by ineffective large-scale culture. hiPSCs were cultured in multilayer culture plates (CPs) with active gas ventilation (AGV), resulting in stable proliferation and pluripotency. Seeding of 1×10^6 hiPSCs per layer yielded 7.2×10^8 hiPSCs in 4-layer CPs and 1.7×10^9 hiPSCs in 10-layer CPs with pluripotency. hiPSCs were sequentially differentiated into cardiomyocytes (CMs) in a two-dimensional (2D) differentiation protocol. The efficiency of cardiac differentiation using 10-layer CPs with AGV was 66%–87%. Approximately $6.2–7.0 \times 10^8$ cells (4-layer) and $1.5–2.8 \times 10^9$ cells (10-layer) were obtained with AGV. After metabolic purification with glucose- and glutamine-depleted and lactate-supplemented media, a massive amount of purified CMs was prepared. Here, we present a scalable 2D culture system using multilayer CPs with AGV for hiPSC-derived CMs, which will facilitate clinical applications for severe heart failure in the near future.

INTRODUCTION

Heart failure (HF) causes high mortality and lack of mobility in developed countries. Currently, heart transplantation is the only radical treatment; however, this treatment approach is limited by donor shortages (Lund et al., 2014). Regenerative medicine represents a promising therapeutic alternative for patients with HF. Human induced pluripotent stem cells (hiPSCs) are an ideal cell source and can be acquired from patient tissues (Takahashi et al., 2007). Small amounts of cells (graft size: 1.3×3 mm^2, cell density: 4,500 < viable cells/mm^2 < 29,000) have been used for the treatment of macular degeneration in the first clinical application of hiPSCs (Mandai et al., 2017). However, more than 1×10^9 hiPSC-derived cardiomyocytes (hiPSC-CMs) would be required to recover cardiac function (Kempf et al., 2016).

Although two-dimensional (2D) static culture systems are suitable for both the maintenance and proliferation of hPSCs, most large-scale culture systems for undifferentiated hPSCs have adopted suspension culture systems (SCSs) (Chen et al., 2014; Serra et al., 2012). The biggest advantages of SCSs are easy scale-up of culture volume and effortless medium changes. Undifferentiated hPSCs in SCSs experience shear stress from the agitation, resulting in heterogeneity and differentiation and leading to deterioration of cell quality; thus, optimizing agitation speed is necessary for each cell line (Singh et al., 2010; Zweigerdt et al., 2011). SCSs are more suitable for generation of differentiated cells, as cell aggregation occurs naturally during embryoid body (EB) differentiation (Hemmi et al., 2014; Kempf et al., 2014; Niebruegge et al., 2009). Methods using microcarriers (MCs) in SCSs are another attractive approach for expansion of hPSCs and CMs (Oh et al., 2009). These SCSs have strong advantages in the scale-up of PSCs and CMs. However, complete elimination of the remaining undifferentiated hPSCs in cell aggregates may not be achieved in SCSs, leading to teratoma formation *in vivo* (Hemmi et al., 2014; Hentze et al., 2009).

To eliminate undifferentiated hPSCs from large-scale cultures of hPSC derivatives, Tohyama et al. (2013) developed metabolic purification. Moreover, 2D cell culture is ideal for high-efficiency generation of pure hiPSC-CMs because all cells are evenly exposed to purification medium (Tohyama et al., 2016).

Here, we report a sequential 2D culture system for the generation of large numbers of pure hiPSC-CMs with high efficiency.

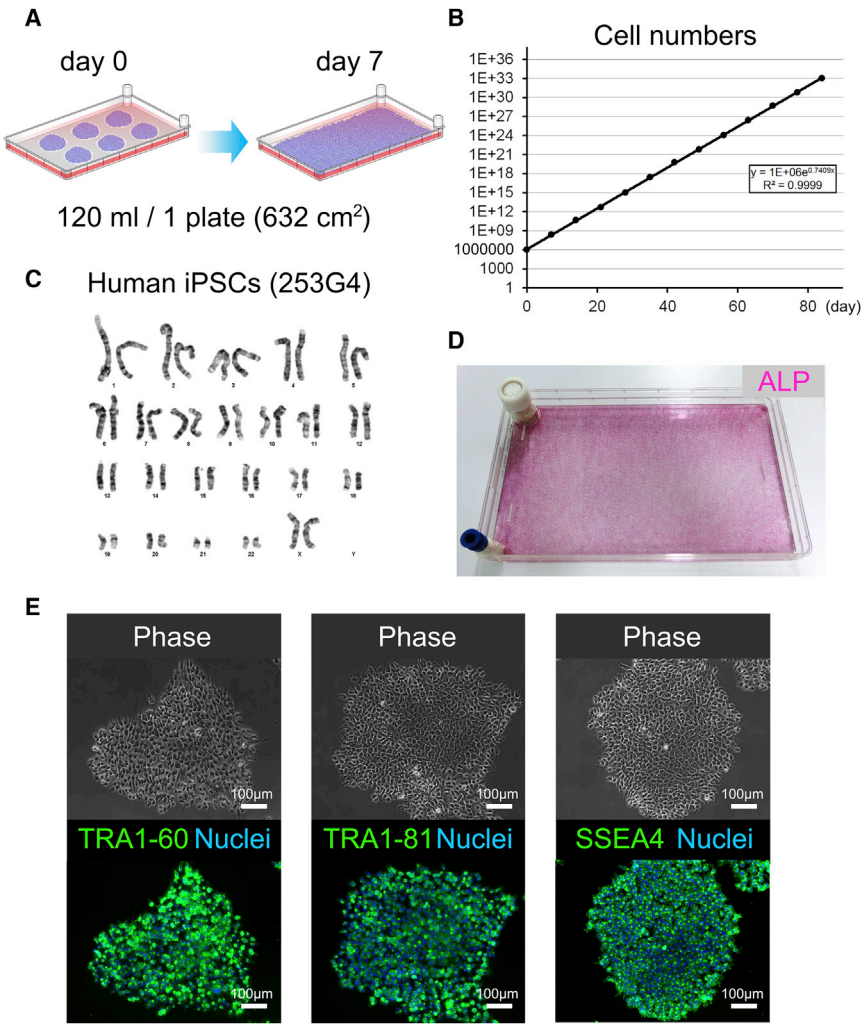

Figure 1. hiPSCs Were Cultured in a Single-Layer CP

(A) Schematic representation of the cell culture in a single-layer CP; the total volume of cells in each plate was 120 mL.

(B) Growth curve of hiPSCs (253G4) in a single-layer CP. Each dot represents a passage of cells.

(C) Karyotype of hiPSCs (253G4) after cell culture in a single-layer CP.

(D) Maintenance of hiPSCs (253G4) in the undifferentiated state as determined by alkaline phosphatase staining.

(E) hiPSC (253G4) expression of the pluripotency markers TRA1-60, TRA1-81, and SSEA4. Scale bars represent 100 μm.

See also Figure S1.

RESULTS

Expansion of hiPSCs in a Single-Layer Culture Plate

We evaluated a large-scale 2D culture system with multilayer culture plates (CPs) and active gas ventilation (AGV) for production of hiPSCs and differentiated CMs. First, hiPSCs (253G4) were passaged in a single-layer CP in a normal gas incubator for 7 days as controls (Figure 1A). The culture area of the plate was 632 cm^2, which is more than 11-fold larger than that of a 10-cm dish (55 cm^2). The proliferation rate was approximately 187-fold (Figure 1B). Upon inoculation of 1×10^6 hiPSCs, approximately 1.9×10^8 hiPSCs were consistently obtained from a confluent single-layer CP over a 7-day period (3.0×10^5 cells/cm^2). The karyotype of the cultured hiPSCs was normal (Figure 1C). The pluripotent state was verified by alkaline phosphatase (AP) staining. All colonies were AP positive, and hiPSCs were evenly cultured throughout the single-layer CP (Figure 1D). Immunofluorescence staining additionally confirmed strong expression of pluripotency markers in all colonies (Figure 1E). These data strongly indicated that the present large-scale 2D culture system was suitable for the maintenance of pluripotency in hiPSCs.

Expansion of hiPSCs in a Multilayer CP with or without AGV

Next, hiPSCs (253G4) were cultured in 4-layer CPs with AGV (Figure S1A). The AGV system enabled the maintenance of 5% carbon dioxide (CO_2) in every layer of a 4- or 10-layer CP. When 4×10^6 hiPSCs were seeded in a 4-layer CP, the number of hiPSCs increased by 179-fold over a 7-day period (Figure S1B). The proliferation efficiency in a 4-layer CP with AGV was almost equal to that of a single-layer CP (Figure S1C). Pluripotency was also confirmed by immunofluorescence staining of NANOG, OCT4, TRA1-60, and SSEA4 (Figure S1D). To evaluate the differences between AGV and normal gas

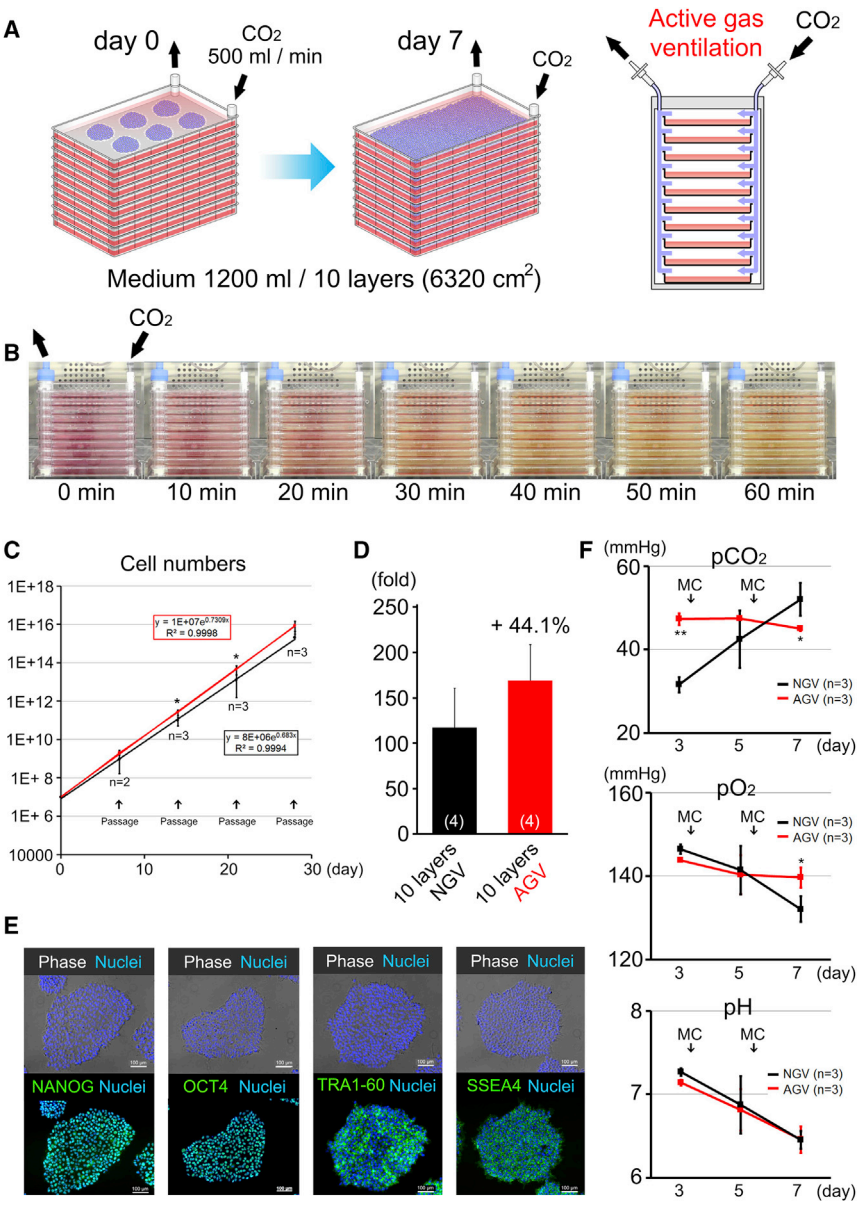

Figure 2. The 10-Layer CP System Was Useful for Acquisition of Large Numbers of hiPSCs

(A) Schematic representation of cell culture in a 10-layer CP under active gas ventilation (AGV); the total volume of medium was 1,200 mL per 10-layer CP.

(B) Rapid conversion of phenol red in the PBS from red to yellow color over a 1-hr period in the AGV system.

(C) Growth curves of hiPSCs (253G4) in a 10-layer CP under normal gas ventilation (NGV, black) or AGV (red). Each dot represents the average cumulative cell numbers in each passage.

(D) Proliferation rates in 10-layer CPs under NGV (n = 4) or AGV (n = 4). Each bar represents the average of the fold changes from individual passages.

(E) hiPSC (253G4) expression of the pluripotency markers NANOG, OCT4, TRA1-60, and SSEA4, as determined by immunofluorescence staining. Scale bars represent 100 μm.

(F) pCO_2, pO_2, and pH levels during cultivation in a 10-layer CP under NGV or AGV (n = 3 independent experiments).

Data are presented as mean ± SD. *p < 0.05; **p < 0.01. See also Figure S2.

ventilation (NGV), we measured the bioprofiles (partial pressure of CO_2 [pCO_2], partial pressure of O_2 [pO_2], pH, glucose, and glutamine) in the culture medium in 4-layer CPs under AGV or NGV (Figure S1E). pCO_2 was stable at each time point under AGV; however, it significantly increased with time under NGV. pH decreased under both conditions. pO_2 was not significantly changed, whereas glucose and glutamine remarkably decreased in hiPSC cultures over time, as reported previously (Tohyama et al., 2013, 2016).

Finally, hiPSCs (253G4) were cultured in 10-layer CPs with AGV (Figure 2A). First, we examined the feasibility of 10-layer CPs with the AGV system. To examine the permeation of CO_2 in each layer, we observed changes in phenol red color in medium over time. Phenol red in PBS rapidly turned from red to yellow after 1 hr in the AGV system (Figure 2B). Next, the gas exchange rate was examined using nitrogen filling. The exchange of air was almost completed in 4 hr using the AGV system (Figure S2A). However, gas exchange could not be completed using the NGV system, even over a 24-hr period (Figure S2B). The proliferation efficiency was also compared between NGV and AGV incubators. The proliferation of hiPSCs with AGV was more stable than that with NGV (Figure 2C). With AGV, the yield was 1.7×10^9 hiPSCs (44% more than under NGV conditions) in the 10-layer CPs over a 7-day period (Figure 2D).

Furthermore, the morphology of hiPSCs was normal, and cells were clearly stained with OCT4, NANOG, SSEA4, and TRA1-60 (Figure 2E). The expression of pluripotent markers was also confirmed by flow-cytometry analysis (Figure S2C). The differences between AGV and NGV in 10-layer CPs were also compared using bioprofiles (Figure 2F). Even in the 10-layer CPs, pCO_2 was more stable at each time point under AGV; however, it was much lower at day 3 and significantly increased with time under NGV. pH decreased under both conditions in the same way as it did in the 4-layer CPs. Unlike in the 4-layer CPs, pO_2 significantly decreased under NGV conditions. Bioprofiles in 10-cm dishes confirmed that pCO_2 in multilayer CPs under AGV was as stable as in ordinary cell culture. Moreover, pO_2 was more stable in multilayer CPs (Figures 2F and S2D). These results indicated that AGV was necessary to culture hiPSCs efficiently in multilayer CPs.

Cardiac Differentiation from hiPSCs in a Multilayer CP with or without AGV

hiPSCs (253G4, 201B7, and FfI14) were sequentially differentiated into CMs from 90% confluent hiPSCs in 4- or 10-layer CPs (Figure 3A). The hiPSC-CMs started to beat at 7–10 days. Cells were collected at day 10 and analyzed by immunofluorescence staining and flow cytometry. Cell viabilities after cardiac differentiation in single-, 4-, or 10-layer CPs under NGV or AGV were over 95% (Figure 3B). Total cell numbers after differentiation derived from hiPSCs (253G4) in single-, 4-, or 10-layer CPs under AGV were 1.5×10^8, 6.7×10^8, and 1.5×10^9, respectively (Figures 3C, S3A, and S3B). Total cell number after differentiation derived from other cell lines (201B7 and FfI14) in a 4-layer CP was $6.2–7.0 \times 10^8$ (Figure S3B). The cardiac differentiation efficiency (253G4 and FfI14) was not significantly different in 10-layer CPs between AGV and NGV (Figures 3D and S3C). In contrast, total hiPSC-CM numbers were higher in AGV than in NGV because proliferative efficiency in lower chambers of 10-layer CPs was low (Figures 3D, S3C, and S3D). The proportion of cardiac troponin T (cTnT)-positive cells derived from hiPSCs (253G4) using 10-layer CPs was approximately 80% (Figure 3E). The differentiated CMs were then enzymatically dissociated and seeded on single-layer CPs or 15-cm dishes. Next, the cells were metabolically selected under glucose- and glutamine-depleted and lactate-supplemented conditions (Tohyama et al., 2016). Expression of the cardiac marker α-actinin was confirmed by immunofluorescence staining (Figures 3F, 3G, and S3E). Flow-cytometry analysis confirmed that following this metabolic selection, almost all cells (>97%) clearly expressed cTnT (Figures 3H, S3F, and S3G; Movie S1). The yield-based efficiency by metabolic selection was 77.5% (Figure S3H), and the viability of the cryopreserved cells after thawing was over 80% (Figure S3I).

Characterization of Metabolically Purified hiPSC-CMs

The characteristics of pure hiPSC-CMs via cryopreservation were analyzed by immunostaining. Most hiPSC-CMs developed into the myosin light chain 2v (MLC2v)-positive ventricular phenotype after metabolic selection (Figure 4A). Electrophysiological characteristics of pure hiPSC-CMs were analyzed by the whole-cell patch-clamp technique and multielectrode array system. The typical action potential of ventricular CMs was recorded, and the results of maximum diastolic potential, action potential amplitude, and action potential duration at 50% of the amplitude supported the ventricular phenotype of pure hiPSC-CMs (Figures 4B and 4C). To assess functional properties, we added isoproterenol to stimulate β-adrenoceptor (Figure 4B). The beating rate increased in a concentration-dependent manner (Figures 4D and 4E). Addition of E-4031 (a water-soluble hERG channel blocker) to pure hiPSC-CMs prolonged field potential duration, a surrogate marker for QT-interval (Figures 4F and 4G). These data confirmed that pure hiPSC-CMs via cryopreservation had normal electrophysiological properties.

DISCUSSION

A serial large-scale cell culture system using multilayer CPs with AGV was established for hiPSCs and differentiated CMs. A clinically necessary number of hiPSC-CMs was efficiently obtained from both 4- and 10-layer CPs. Finally, the cells were refined by metabolic selection.

Although the cardiac differentiation protocol was reformed, the cardiac differentiation efficiency from hiPSCs depends on the cell line, and such procedures often produce hiPSC-CMs with low efficiency (Mummery et al., 2012). Moreover, hiPSC-CMs exhibit a fetal phenotype and gradually lose proliferative capacity after cardiac differentiation over time (Zhang et al., 2009). Therefore, the large number of hiPSCs present is a major premise for obtaining hiPSC-CMs on a large scale.

In previous studies, 2D monolayer culture was established as a conventional culture system for undifferentiated hPSCs (Takahashi et al., 2007; Thomson et al., 1998). This standard culture method has the advantage of maintaining the pluripotent state and high differentiation potential. Moreover, 2D monolayer culture is also advantageous for cardiac differentiation because all cells are uniformly exposed to medium, including growth factors, small molecules, and paracrine factors (Lian et al., 2013; Mummery et al., 2012). The main disadvantage of 2D culture systems is low cell yield due to the limited surface area. Thus, 2D culture systems usually need "scale out" to acquire large amounts of cells; this necessitates substantial space and labor (Kempf et al., 2016). Multilayer CPs overcame these

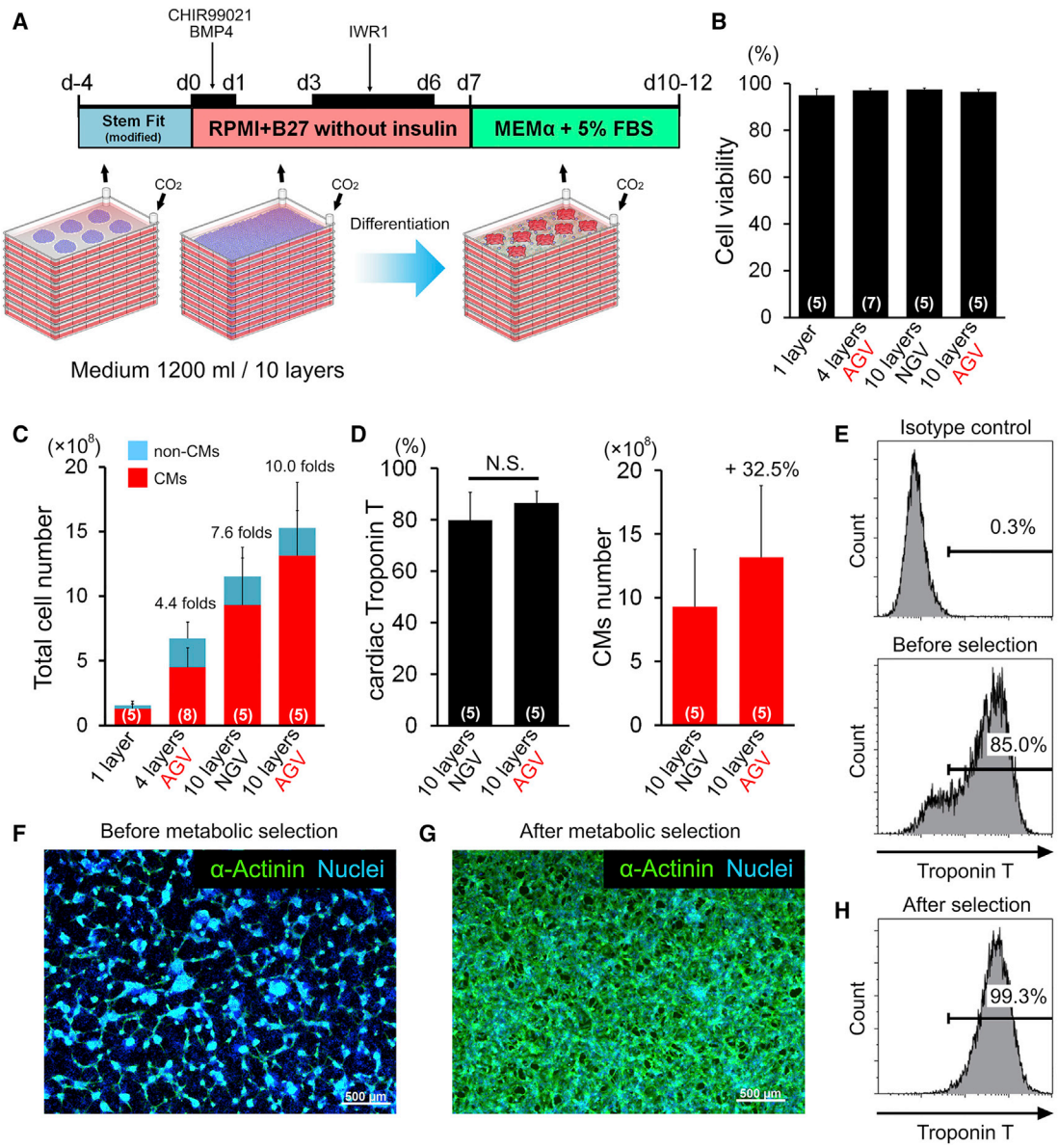

Figure 3. Large-Scale Culture of Cardiac Differentiation from hiPSCs in a Multilayer CP

(A) Schematic representation of the cardiac differentiation protocol. The expanded hiPSCs were successively cultured for cardiac differentiation in 4- or 10-layer CPs. d, day; FBS, fetal bovine serum.

(B) The bar graphs show cell viability after cardiac differentiation from hiPSCs (253G4) in single-layer (n = 5), 4-layer (n = 7), or 10-layer (n = 5) CPs under NGV or AGV. Data were obtained from independent experiments.

(C) Total cell number of hiPSC (253G4)-derived cells in single-layer (n = 5), 4-layer (n = 8), or 10-layer (n = 5) CPs under NGV or AGV. Data were obtained from independent experiments.

(D) The proportion and final yield of troponin T-positive cardiomyocytes (CMs) derived from hiPSCs (253G4) in 10-layer CPs under NGV or AGV (n = 5 independent experiments). N.S., not significant.

(E) Representative flow-cytometry analysis for troponin T-positive cells in 10-layer CPs under AGV.

(F and G) Representative immunofluorescence staining for α-actinin (green) and nuclei (blue) in hiPSC (253G4)-derived dispersed cells before (F) and after (G) metabolic selection. Scale bars represent 500 μm.

(H) Representative flow-cytometry analysis for troponin T-positive cells after metabolic selection.

Data are presented as mean ± SD. See also Figure S3.

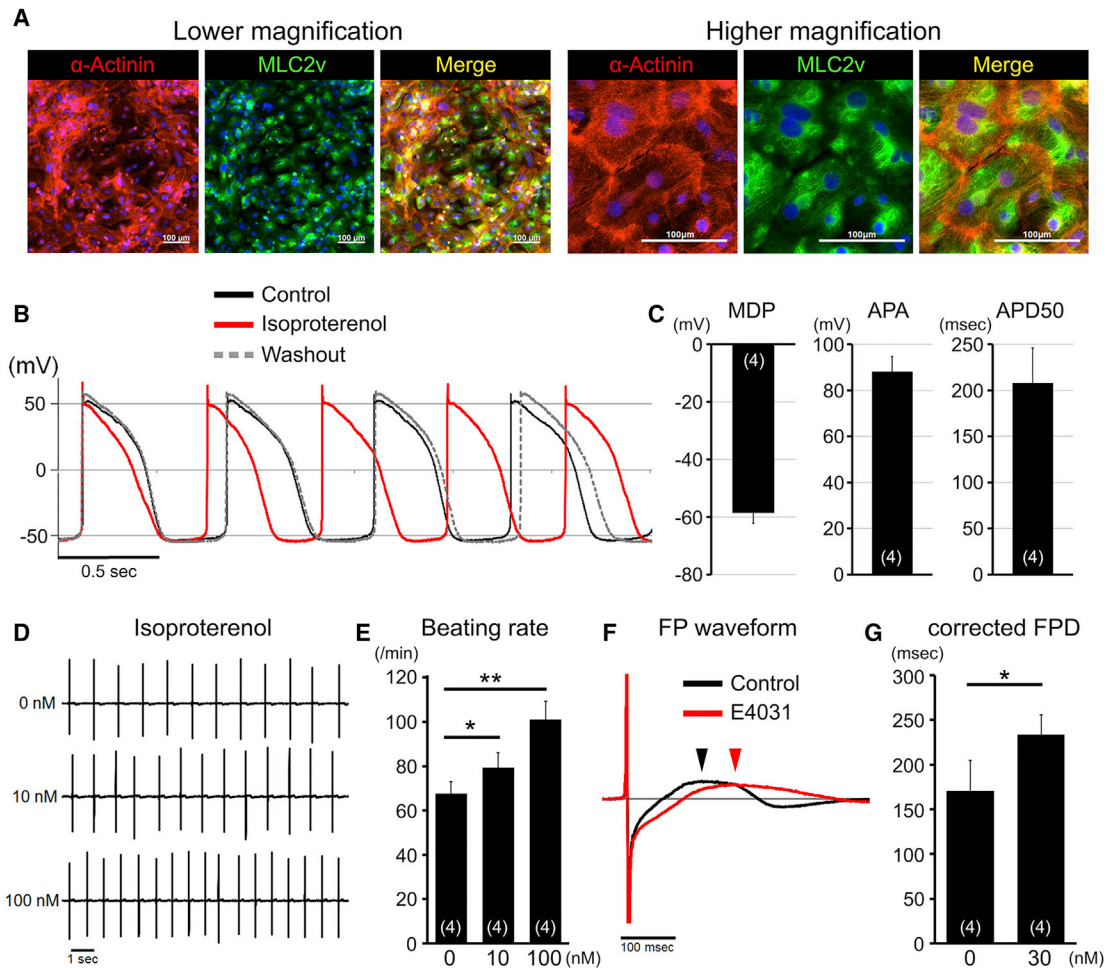

Figure 4. Electrophysiological Properties of Purified hiPSC-CMs

(A) Immunofluorescence staining for α-actinin (red), MLC2v (green), and nuclei (blue) in purified hiPSC (253G4)-CMs after thawing. Scale bars represent 100 μm.

(B) Metabolically purified CMs after thawing showed ventricular-like action potentials (n = 4 independent experiments) and responded to isoproterenol (10 nM) administration.

(C) The bar graphs show maximum diastolic potential (MDP), action potential amplitude (APA), and action potential duration at 50% of the amplitude (APD50) in metabolically purified CM after thawing (n = 4 independent experiments). Data are presented as mean ± SEM.

(D) Representative field potentials (FPs) in metabolically purified CMs with or without isoproterenol administration.

(E) The graph summarizes changes in beating rates with or without isoproterenol administration (n = 4 independent experiments). Data are presented as mean ± SD.

(F) Representative FPs in metabolically purified CM with or without E4031 administration.

(G) The graph summarizes changes in corrected field potential duration (FPD) with or without E4031 administration (n = 4 independent experiments). Data are presented as mean ± SD.

*p < 0.05; **p < 0.01.

problems (Schulz et al., 2012), but it was difficult to maintain the CO_2 concentration in each layer evenly in NGV. Fluctuation of CO_2 concentration could affect cell behavior; highly elevated CO_2 levels cause mitochondrial dysfunction and impair cell proliferation regardless of acidosis (Vohwinkel et al., 2011). Recently, it was reported that mitochondrial oxidative phosphorylation played an important role in survival and proliferation of hiPSCs as well as hiPSC-CMs (Tohyama et al., 2016). Therefore, one reason for the efficient culture of hiPSCs and hiPSC-CMs that we observed using multilayer CPs may be the stable maintenance of pO_2 and pCO_2 allowed by AGV.

Other disadvantages of the 2D culture system are cell harvesting and the lack of control of important culture parameters. Cell harvesting is relatively difficult from multilayer CPs in comparison with single-layer CPs. In our

experiments, hiPSC recovery from 4-layer CPs was almost same as that of hiPSCs from single-layer CPs (Figure S1C). However, cell recovery in 10-layer CPs with AGV was estimated to be approximately 90% (Figures S1C and 2D). The total cell yield of 10-layer CPs outweighed this cell loss; however, this problem should be addressed in future studies to improve efficiency. Monitoring of culture conditions is also necessary in future studies of large-scale 2D culture systems using multilayer CPs.

The scalable culture system for hPSCs was mainly researched using SCSs (Chen et al., 2014; Krawetz et al., 2010; Silva et al., 2015). The shear stress caused by agitation can affect both pluripotency of hiPSCs and differentiation potential. If spheroid-formed hPSCs in SCSs are not maintained appropriately, they are at high risk of losing pluripotency and developing into EBs (Krawetz et al., 2010; Singh et al., 2010). Particularly with regard to clinical applications, it would be difficult to evaluate the undifferentiated state by observation of hiPSC morphology.

SCSs for somatic differentiation were more common in hPSC culture and were also effective for cardiac development (Hemmi et al., 2014; Kempf et al., 2014; Niebruegge et al., 2009). When stirred conditions (agitation speed, impeller type, cell density) are appropriately adjusted, cells are easily scaled up, and culture conditions can be monitored with a bioreactor (Kempf et al., 2014; Olmer et al., 2012). However, there is a high possibility that residual undifferentiated hPSCs exist in the EBs. We developed a metabolic selection system with glucose- and glutamine-depleted as well as lactate-supplemented conditions for expansion of clinical-grade hiPSC-CMs (Tohyama et al., 2016). For clinical applications, the remaining hPSCs in EBs are much more difficult to completely eliminate during purification because they stick to each other, and the purification medium may not reach the cells on the inside of the clumps. If cell aggregates are forced to dissociate, they lose the viability. In contrast, cardiac differentiation in 2D culture was efficient and made it easier to observe cellular status and achieve purification.

MCs are another unique large-scale culture system providing sufficient surface area for cell adhesion in SCSs. MCs were used in static conditions and applied to stirred SCSs (Oh et al., 2009). Recently, serum-free and xeno-free SCSs with MCs also became available (Badenes et al., 2016a; Lam et al., 2014a). Despite using MCs, some PSC lines exhibit unavoidable shear stress in stirred SCSs (Leung et al., 2011). Lower shear stress results in highly efficient cardiac differentiation (Ting et al., 2014). MC type, aggregation size, and MC coating are also important for scalable expansion and controlled differentiation of hPSCs (Lam et al., 2014b; Lecina et al., 2010). Cost-effective, xeno-free, and synthetic, dissolvable MCs using non-proteolytic enzymes must be developed for clinical translation (Badenes et al., 2016b; Chen et al., 2014).

In summary, an efficient scalable 2D culture system was developed for the serial culture of undifferentiated hiPSCs until cardiac differentiation. Furthermore, the metabolic selection system enabled successful purification of the expanded hiPSC-CMs. This innovative massive culture system will be useful for generating a large number of hiPSC-CMs with high efficiency for clinical applications.

EXPERIMENTAL PROCEDURES

Measurement of pCO_2, pO_2, pH, and Metabolites in Culture Medium

Under AGV and NGV, pCO_2, pO_2, pH, glucose, and glutamine levels in the medium were measured using a BioProfile 400 Analyzer (Nova Biomedical, USA) during the maintenance and cultivation of hiPSCs using the multilayer CPs or 10-cm culture dishes.

SUPPLEMENTAL INFORMATION

Supplemental Information includes Supplemental Experimental Procedures, three figures, and one movie and can be found with this article online at http://dx.doi.org/10.1016/j.stemcr.2017.08.025.

AUTHOR CONTRIBUTIONS

S. Tohyama and J.F. conceived the study; S. Tohyama, C.F., M.Y., S. Kanaami, and R.O. performed the experiments; K.S., M.K., and J.K. performed the electrophysiological experiments; S. Tohyama, J.F., H.K., T.S., Y.K., and M.O. analyzed the data; S. Tanosaki and S.S. designed the methodology; K.N., A.H., and S. Kawaguchi contributed to specific experiments; J.F. and S. Tohyama wrote the manuscript; J.F., E.K., and K.F. supervised the study.

ACKNOWLEDGMENTS

The authors thank the Center for iPSC Research and Application, Kyoto University, for providing the 253G4, 201B7, and Ff114 hiPSC lines. This work was supported by the Highway Program for Realization of Regenerative Medicine from the Japan Science and Technology Agency (no. 16bm0504006h0006 to K.F.) and partly supported by the Support Program to Break the Bottlenecksat R&D for Accelerating the Practical Use of Health Research Outcomes (no. 34201006-01 to K.F.), a Japan Society for the Promotion of Science JSPS KAKENHI grant (no. 16K09507 to J.F., no. 15H04684 to J.K., and no. 15K09098 to H.K.), and the SENSHIN Medical Research Foundation (to S. Tohyama). The authors are grateful to Satoru Okamoto, Yusuke Natsume, and Kotoe Terasawa for providing the medium (Ajinomoto Co., Inc.) and to Yoshihide Miyatani and Akira Yamamoto for adjusting the incubators with the AGV system (Taitec Corporation). K.F., who is a co-founder of Heartseed, Inc., has equity in Heartseed, Inc.

Received: December 11, 2016
Revised: August 30, 2017
Accepted: August 31, 2017
Published: October 5, 2017

REFERENCES

Badenes, S.M., Fernandes, T.G., Cordeiro, C.S., Boucher, S., Kuninger, D., Vemuri, M.C., Diogo, M.M., and Cabral, J.M. (2016a). Defined essential 8 medium and vitronectin efficiently support scalable xeno-free expansion of human induced pluripotent stem cells in stirred microcarrier culture systems. PLoS One *11*, e0151264.

Badenes, S.M., Fernandes, T.G., Rodrigues, C.A., Diogo, M.M., and Cabral, J.M. (2016b). Microcarrier-based platforms for in vitro expansion and differentiation of human pluripotent stem cells in bioreactor culture systems. J. Biotechnol. *234*, 71–82.

Chen, K.G., Mallon, B.S., McKay, R.D., and Robey, P.G. (2014). Human pluripotent stem cell culture: considerations for maintenance, expansion, and therapeutics. Cell Stem Cell *14*, 13–26.

Hemmi, N., Tohyama, S., Nakajima, K., Kanazawa, H., Suzuki, T., Hattori, F., Seki, T., Kishino, Y., Hirano, A., Okada, M., et al. (2014). A massive suspension culture system with metabolic purification for human pluripotent stem cell-derived cardiomyocytes. Stem Cells Transl. Med. *3*, 1473–1483.

Hentze, H., Soong, P.L., Wang, S.T., Phillips, B.W., Putti, T.C., and Dunn, N.R. (2009). Teratoma formation by human embryonic stem cells: evaluation of essential parameters for future safety studies. Stem Cell Res. *2*, 198–210.

Kempf, H., Andree, B., and Zweigerdt, R. (2016). Large-scale production of human pluripotent stem cell derived cardiomyocytes. Adv. Drug Deliv. Rev. *96*, 18–30.

Kempf, H., Olmer, R., Kropp, C., Ruckert, M., Jara-Avaca, M., Robles-Diaz, D., Franke, A., Elliott, D.A., Wojciechowski, D., Fischer, M., et al. (2014). Controlling expansion and cardiomyogenic differentiation of human pluripotent stem cells in scalable suspension culture. Stem Cell Reports *3*, 1132–1146.

Krawetz, R., Taiani, J.T., Liu, S., Meng, G., Li, X., Kallos, M.S., and Rancourt, D.E. (2010). Large-scale expansion of pluripotent human embryonic stem cells in stirred-suspension bioreactors. Tissue Eng. Part C Methods *16*, 573–582.

Lam, A.T., Chen, A.K., Li, J., Birch, W.R., Reuveny, S., and Oh, S.K. (2014a). Conjoint propagation and differentiation of human embryonic stem cells to cardiomyocytes in a defined microcarrier spinner culture. Stem Cell Res. Ther. *5*, 110.

Lam, A.T., Li, J., Chen, A.K., Reuveny, S., Oh, S.K., and Birch, W.R. (2014b). Cationic surface charge combined with either vitronectin or laminin dictates the evolution of human embryonic stem cells/microcarrier aggregates and cell growth in agitated cultures. Stem Cells Dev. *23*, 1688–1703.

Lecina, M., Ting, S., Choo, A., Reuveny, S., and Oh, S. (2010). Scalable platform for human embryonic stem cell differentiation to cardiomyocytes in suspended microcarrier cultures. Tissue Eng. Part C Methods *16*, 1609–1619.

Leung, H.W., Chen, A., Choo, A.B., Reuveny, S., and Oh, S.K. (2011). Agitation can induce differentiation of human pluripotent stem cells in microcarrier cultures. Tissue Eng. Part C Methods *17*, 165–172.

Lian, X., Zhang, J., Azarin, S.M., Zhu, K., Hazeltine, L.B., Bao, X., Hsiao, C., Kamp, T.J., and Palecek, S.P. (2013). Directed cardiomyocyte differentiation from human pluripotent stem cells by modulating Wnt/beta-catenin signaling under fully defined conditions. Nat. Protoc. *8*, 162–175.

Lund, L.H., Edwards, L.B., Kucheryavaya, A.Y., Benden, C., Christie, J.D., Dipchand, A.I., Dobbels, F., Goldfarb, S.B., Levvey, B.J., Meiser, B., et al. (2014). The registry of the International Society for Heart and Lung Transplantation: thirty-first official adult heart transplant report—2014; focus theme: retransplantation. J. Heart Lung Transplant. *33*, 996–1008.

Mandai, M., Watanabe, A., Kurimoto, Y., Hirami, Y., Morinaga, C., Daimon, T., Fujihara, M., Akimaru, H., Sakai, N., Shibata, Y., et al. (2017). Autologous induced stem-cell-derived retinal cells for macular degeneration. N. Engl. J. Med. *376*, 1038–1046.

Mummery, C.L., Zhang, J., Ng, E.S., Elliott, D.A., Elefanty, A.G., and Kamp, T.J. (2012). Differentiation of human embryonic stem cells and induced pluripotent stem cells to cardiomyocytes: a methods overview. Circ. Res. *111*, 344–358.

Niebruegge, S., Bauwens, C.L., Peerani, R., Thavandiran, N., Masse, S., Sevaptisidis, E., Nanthakumar, K., Woodhouse, K., Husain, M., Kumacheva, E., et al. (2009). Generation of human embryonic stem cell-derived mesoderm and cardiac cells using size-specified aggregates in an oxygen-controlled bioreactor. Biotechnol. Bioeng. *102*, 493–507.

Oh, S.K., Chen, A.K., Mok, Y., Chen, X., Lim, U.M., Chin, A., Choo, A.B., and Reuveny, S. (2009). Long-term microcarrier suspension cultures of human embryonic stem cells. Stem Cell Res. *2*, 219–230.

Olmer, R., Lange, A., Selzer, S., Kasper, C., Haverich, A., Martin, U., and Zweigerdt, R. (2012). Suspension culture of human pluripotent stem cells in controlled, stirred bioreactors. Tissue Eng. Part C Methods *18*, 772–784.

Schulz, T.C., Young, H.Y., Agulnick, A.D., Babin, M.J., Baetge, E.E., Bang, A.G., Bhoumik, A., Cepa, I., Cesario, R.M., Haakmeester, C., et al. (2012). A scalable system for production of functional pancreatic progenitors from human embryonic stem cells. PLoS One *7*, e37004.

Serra, M., Brito, C., Correia, C., and Alves, P.M. (2012). Process engineering of human pluripotent stem cells for clinical application. Trends Biotechnol. *30*, 350–359.

Silva, M.M., Rodrigues, A.F., Correia, C., Sousa, M.F., Brito, C., Coroadinha, A.S., Serra, M., and Alves, P.M. (2015). Robust expansion of human pluripotent stem cells: integration of bioprocess design with transcriptomic and metabolomic characterization. Stem Cells Transl. Med. *4*, 731–742.

Singh, H., Mok, P., Balakrishnan, T., Rahmat, S.N., and Zweigerdt, R. (2010). Up-scaling single cell-inoculated suspension culture of human embryonic stem cells. Stem Cell Res. *4*, 165–179.

Takahashi, K., Tanabe, K., Ohnuki, M., Narita, M., Ichisaka, T., Tomoda, K., and Yamanaka, S. (2007). Induction of pluripotent stem cells from adult human fibroblasts by defined factors. Cell *131*, 861–872.

Thomson, J.A., Itskovitz-Eldor, J., Shapiro, S.S., Waknitz, M.A., Swiergiel, J.J., Marshall, V.S., and Jones, J.M. (1998). Embryonic

stem cell lines derived from human blastocysts. Science *282*, 1145–1147.

Ting, S., Chen, A., Reuveny, S., and Oh, S. (2014). An intermittent rocking platform for integrated expansion and differentiation of human pluripotent stem cells to cardiomyocytes in suspended microcarrier cultures. Stem Cell Res. *13*, 202–213.

Tohyama, S., Fujita, J., Hishiki, T., Matsuura, T., Hattori, F., Ohno, R., Kanazawa, H., Seki, T., Nakajima, K., Kishino, Y., et al. (2016). Glutamine oxidation is indispensable for survival of human pluripotent stem cells. Cell Metab. *23*, 663–674.

Tohyama, S., Hattori, F., Sano, M., Hishiki, T., Nagahata, Y., Matsuura, T., Hashimoto, H., Suzuki, T., Yamashita, H., Satoh, Y., et al. (2013). Distinct metabolic flow enables large-scale purification of mouse and human pluripotent stem cell-derived cardiomyocytes. Cell Stem Cell *12*, 127–137.

Vohwinkel, C.U., Lecuona, E., Sun, H., Sommer, N., Vadasz, I., Chandel, N.S., and Sznajder, J.I. (2011). Elevated CO(2) levels cause mitochondrial dysfunction and impair cell proliferation. J. Biol. Chem. *286*, 37067–37076.

Zhang, J., Wilson, G.F., Soerens, A.G., Koonce, C.H., Yu, J., Palecek, S.P., Thomson, J.A., and Kamp, T.J. (2009). Functional cardiomyocytes derived from human induced pluripotent stem cells. Circ. Res. *104*, e30–e41.

Zweigerdt, R., Olmer, R., Singh, H., Haverich, A., and Martin, U. (2011). Scalable expansion of human pluripotent stem cells in suspension culture. Nat. Protoc. *6*, 689–700.

Stem Cell Reports, Volume *9*

Supplemental Information

Efficient Large-Scale 2D Culture System for Human Induced Pluripotent Stem Cells and Differentiated Cardiomyocytes

Shugo Tohyama, Jun Fujita, Chihana Fujita, Miho Yamaguchi, Sayaka Kanaami, Rei Ohno, Kazuho Sakamoto, Masami Kodama, Junko Kurokawa, Hideaki Kanazawa, Tomohisa Seki, Yoshikazu Kishino, Marina Okada, Kazuaki Nakajima, Sho Tanosaki, Shota Someya, Akinori Hirano, Shinji Kawaguchi, Eiji Kobayashi, and Keiichi Fukuda

Figure S1

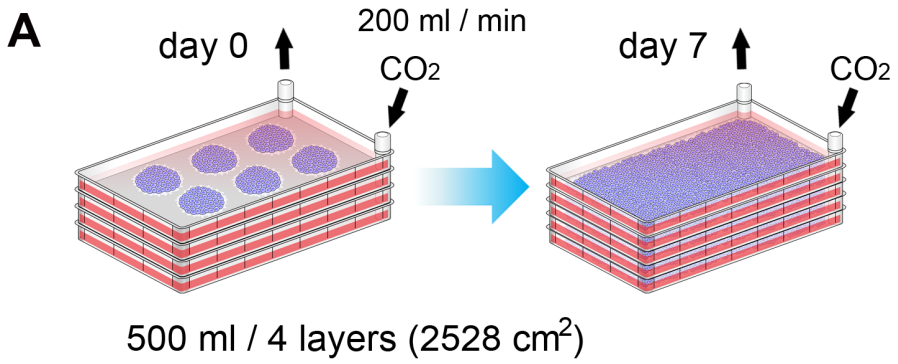
A
day 0
200 ml / min
CO2
day 7
CO2
500 ml / 4 layers (2528 cm2)

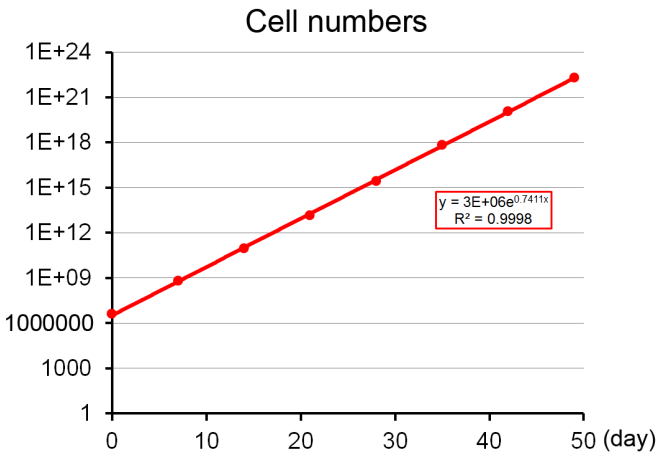
B
Cell numbers
1E+24
1E+21
1E+18
1E+15
1E+12
1E+09
1000000
1000
1
y = 3E+06e0.7411x
R² = 0.9998
0
10
20
30
40
50 (day)

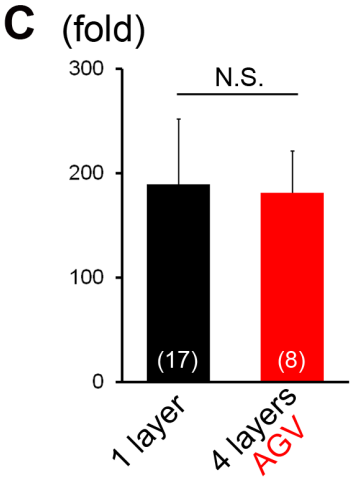
C
(fold)
300
200
100
0
N.S.
(17)
(8)
1 layer
4 layers AGV

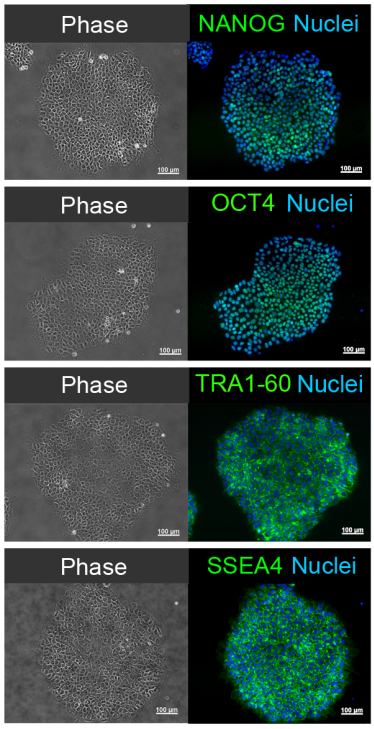
D
Phase
NANOG Nuclei
Phase
OCT4 Nuclei
Phase
TRA1-60 Nuclei
Phase
SSEA4 Nuclei

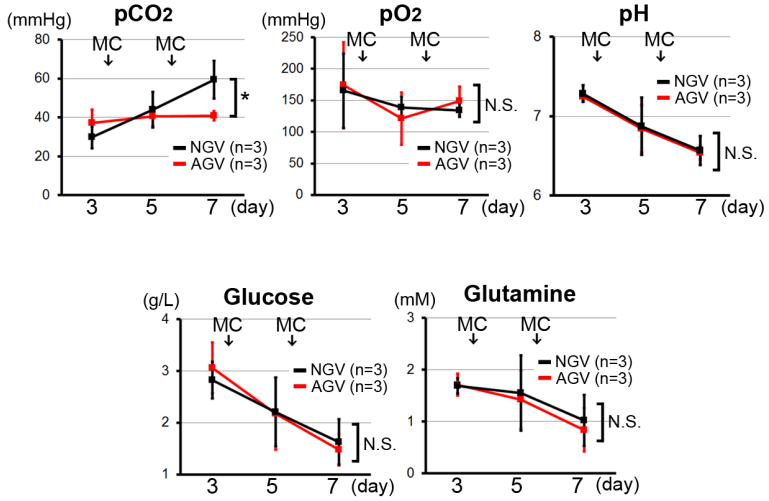
E
(mmHg)
pCO2
MC
MC
NGV (n=3)
AGV (n=3)
*
(day)
(mmHg)
pO2
N.S.
pH
(g/L)
Glucose
(mM)
Glutamine

Figure S2

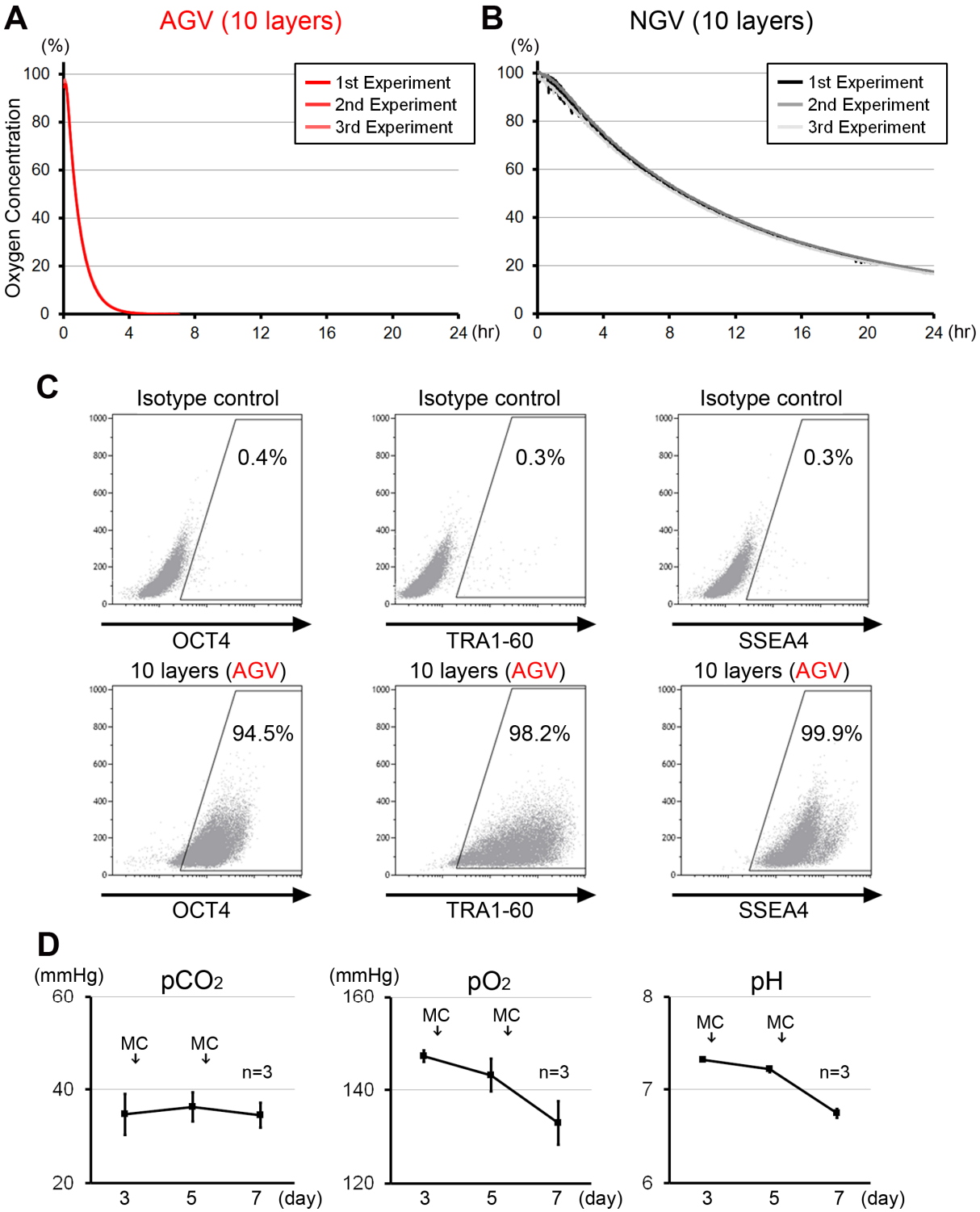
A
AGV (10 layers)
(%)
Oxygen Concentration
1st Experiment
2nd Experiment
3rd Experiment
24 (hr)
B
NGV (10 layers)
C
Isotype control
0.4%
0.3%
OCT4
TRA1-60
SSEA4
10 layers (AGV)
94.5%
98.2%
99.9%
D
pCO2
pO2
pH
(mmHg)
MC
n=3
(day)

Figure S3

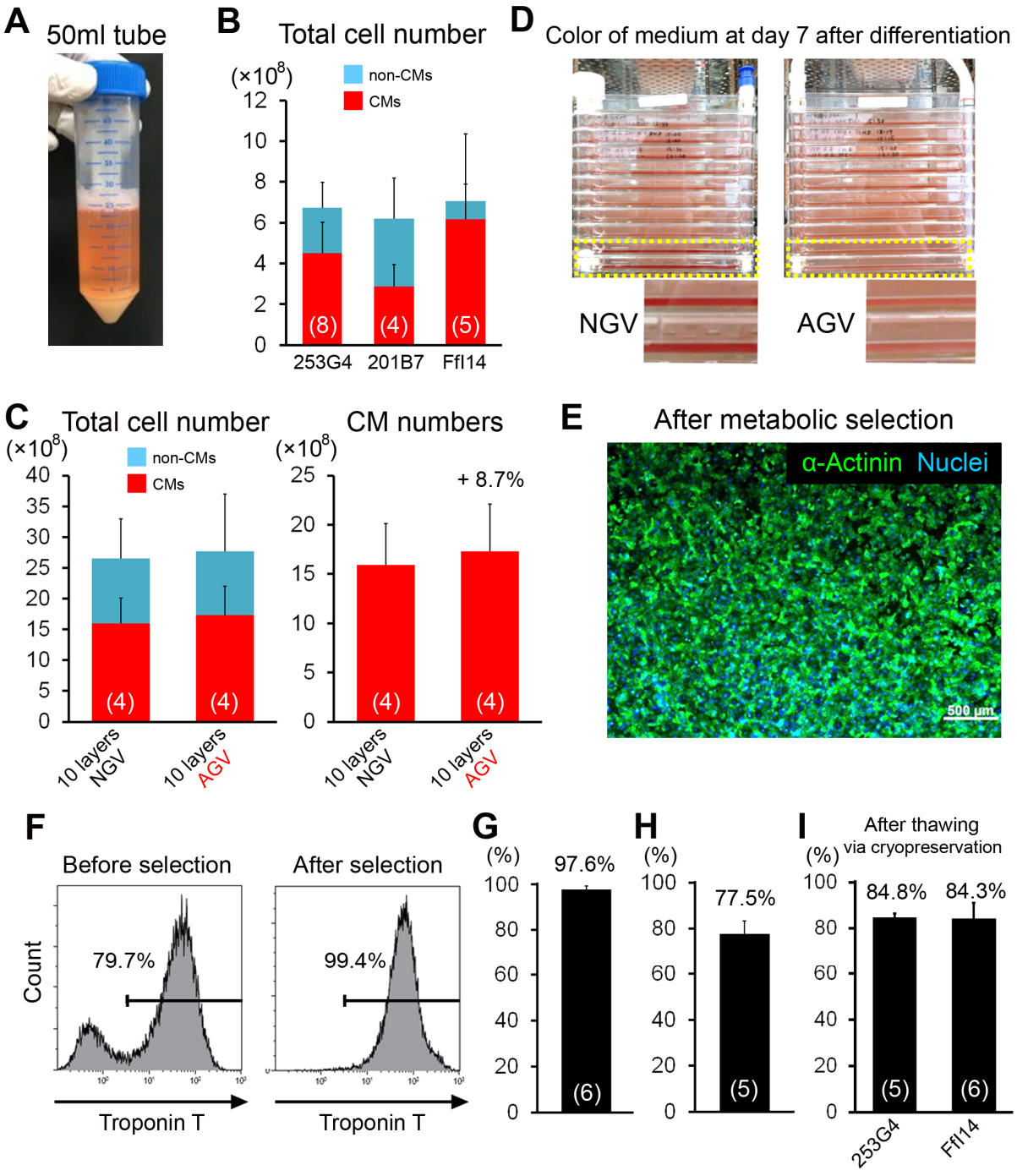
A
50ml tube
B
Total cell number
(×10^8)
non-CMs
CMs
12
10
8
6
4
2
0
(8)
(4)
(5)
253G4
201B7
Ffl14
D
Color of medium at day 7 after differentiation
NGV
AGV
C
Total cell number
(×10^8)
non-CMs
CMs
40
35
30
25
20
15
10
5
0
(4)
(4)
10 layers NGV
10 layers AGV
CM numbers
(×10^8)
25
20
15
10
5
0
+ 8.7%
(4)
(4)
10 layers NGV
10 layers AGV
E
After metabolic selection
α-Actinin Nuclei
500 μm
F
Before selection
After selection
Count
79.7%
99.4%
Troponin T
Troponin T
G
(%)
97.6%
100
80
60
40
20
0
(6)
H
(%)
77.5%
100
80
60
40
20
0
(5)
I
After thawing via cryopreservation
(%)
84.8%
84.3%
100
80
60
40
20
0
(5)
(6)
253G4
Ffl14

SUPPLEMENTAL FIGURE LEGENDS

Figure S1. hiPSCs were cultured in a four-layer CP under AGV, related to Figure 1.

(**A**) The scheme of cell culture in a four-layer CP under AGV. The total volume of medium was 500 mL/CP. (**B**) Growth curve of hiPSCs (253G4) in a four-layer CP. Each dot represents a passage of cells. (**C**) The proliferation rate in a four-layer CP (n = 8) under AGV was as much as that in a single layer CP (n = 17). Each bar represents the fold changes from individual passages. (**D**) Immunofluorescent staining showed that hiPSCs expressed the pluripotent markers NANOG, OCT4, TRA1-60, and SSEA4. Bars are 100 μm. (**E**) pCO_2, pO_2, pH, and the concentrations of glucose and glutamine during cultivation in a four-layer CP under NGV or AGV (n = 3 independent experiments). Data are presented as means ± SD. $*p < 0.05$

Figure S2. The AGV system was more efficient for gas exchange than NGV in a 10-layer CP, related to Figure 2.

(**A and B**) Oxygen concentration was measured in the fifth layer of the 10-layer CP under AGV (**A**) and NGV (**B**). (**C**) FACS analyses of pluripotent markers in hiPSCs cultured using 10-layer CPs under AGV. (**D**) pCO_2, pO_2, and pH levels during cultivation in a 10-cm culture dish under NGV (n = 3 independent experiments).

Figure S3. Large-scale culture of cardiac differentiation from hiPSCs in a multilayer CP, related to Figure 3.

(**A**) A pellet of the hiPSC (253G4)-derived cells cultured using one four-layer CP under AGV. (**B**) Total cell number of hiPSC-derived cells in four-layer CPs under AGV (253G4; n = 8, 201B7; n = 4, Ff‌I14; n = 5). Data were obtained from independent experiments. (**C**) Total cell numbers and cardiomyocyte (CM) numbers of hiPSC (Ff‌I14)-derived cells in 10-layer

CPs under NGV or AGV (n = 4 independent experiments). (**D**) Color of medium in hiPSC-derived cells cultured using 10-layer CPs under NGV (left) or AGV (right). (**E**) Representative immunofluorescence staining for α-actinin (green) and nuclei (blue) in hiPSC (FfI14)-derived dispersed cells after metabolic selection. (**F**) Representative FACS analysis for troponin T-positive cells in hiPSC (FfI14)-derived cells before (left) and after (right) metabolic selection. (**G**) The proportion of troponin T-positive CMs in hiPSC (FfI14)-derived dispersed cells after metabolic selection (n = 6 independent experiments). (**H**) Yield-based efficiencies by metabolic selection (n = 5 independent experiments). (**I**) The bar graphs show viability of cryopreserved hiPSC-derived pure cardiomyocytes after thawing (253G4; n = 5, FfI14; n = 6). Data were obtained from independent experiments. Scale bars represent 500 μm (**E**). Data are presented as means ± SD.

Movie S1. Purified hiPSC-derived dispersed CMs, related to Figure 3.

After differentiation using four-layer CPs, hiPSC (253G4)-derived cells were dissociated and seeded on fibronectin-coated single-layer CPs. Then, the cells were metabolically selected under glucose- and glutamine-depleted conditions in the presence of lactate and reseeded.

SUPPLEMENTAL EXPERIMENTAL PROCEDURES

Maintenance of hiPSCs using single- or multilayer CPs

The hiPSC lines (253G4, 201B7, and FfI14) were obtained from the Center for iPSC Research and Application, Kyoto University. hiPSCs were maintained in modified Stem Fit Medium (Ajinomoto Co., Inc., Japan) on growth factor-reduced Matrigel-coated single- or multilayer (four- or 10-layer) CPs (Thermo Fisher Scientific, USA). In the active gas ventilation (AGV) system, 50 mL/min 5% CO_2 per layer was actively ventilated using a multi-gas incubator (MG-70M; TAITEC Corporation, Japan). hiPSCs were routinely passaged every week using Accutase (Thermo Scientific). Briefly, cells were washed with D-PBS and incubated with Accutase at 37°C. After incubation, cells were collected and reseeded in modified Stem Fit Medium (Ajinomoto) with 10 μM Y27632 (Wako Pure Chemicals, Japan) on growth factor-reduced Matrigel-coated (BD Biosciences, Japan) culture plates. Media were changed every other day (Nakagawa et al., 2014). The number of dissociated single cells was counted using a Vi-Cell cell counter (Beckman Coulter, USA). Karyotypes of hiPSCs were analyzed by Nihon Gene Research Laboratories, Inc. (Sendai, Japan, http://www.ngrljapan.com).

2D cardiomyocyte differentiation using multilayer CPs with NGV or AGV

hiPSCs (1.5×10^7 cells/layer) were seeded in modified Stem Fit Medium (Ajinomoto) on Matrigel-coated multilayer CPs (4 or 10 layers) with NGV or AGV on day -4. When the cells reached 90% confluence on day 0, the medium was changed to RPMI (Wako) with B27 minus insulin (Thermo Scientific), 6 μM CHIR99021 (Wako), and 1 ng/mL bone morphogenic protein 4 (R&D Systems) from day 0 to day 1, as previously reported (Lian et al., 2012; Tohyama et al., 2016), with modifications. The medium was changed to RPMI with B27 minus insulin on day 1. On day 3, the medium was changed to RPMI with B27 minus

insulin and 5 μM IWR1 (Sigma-Aldrich, USA). On day 6, the medium was changed to RPMI with B27 minus insulin. Cells were maintained in MEMα plus 5% fetal bovine serum (FBS; Hyclone) on day 7. From day 7 onwards, the medium was changed every 3–7 days. At day 10 after differentiation, the number of dissociated single cells and cell viability were evaluated by trypan blue staining using a ViCell (Beckman Coulter). Differentiation efficiencies were analyzed using fluorescence-assisted cell sorting (FACS) analysis (Gallios; Beckman Coulter).

Purification of hiPSC-CMs by metabolic selection system

On differentiation days 12–14, hiPSC-derived cells were incubated with D-PBS to remove RPMI with B27 plus insulin for 3 min and then enzymatically dissociated using 0.25% Trypsin-EDTA (Nacalai Tesque). Dissociated cells were collected and seeded on collagen type 1- (IWAKI, Japan) or fibronectin-coated (Sigma) 15 cm dishes or fibronectin-coated single-layer CPs (Thermo Scientific) using MEMα plus 5% FBS. After 1-2 days of cultivation using MEMα plus 5% FBS, hiPSC-derived cells were incubated with D-PBS to remove MEMα plus 5% FBS for 3 min, and the medium was then changed to glucose and glutamine-free DMEM (Ajinomoto) supplemented with 4 mM L-lactic acid and 0.1% BSA (Thermo Scientific) for 3–6 days, as reported previously (Tohyama et al., 2016). The medium was changed every 2 or 3 days to eliminate dead cells. After metabolic selection, purified hiPSC-CMs were cryopreserved or used for immunostaining and FACS analysis.

Components of modified StemFit

In this study, we used modified StemFit medium manufactured by Ajinomoto Co., Inc. As well as StemFit medium (Nakagawa et al., 2014), modified StemFit medium containing 21 amino acids (L-alanine, L-arginine, L-asparagine, L-aspartic acid, L-cysteine, L-cyctine, L-

glutamic acid, L-glutamine, glycine, L-histidine, L-isoleucine, L-leucine, L-lysine, L-methionine, L-phenylalanine, L-proline, L-serine, L-threonine, L-tryptophan, L-tyrosine, and L-valine), 10 vitamins (L-ascorbic acid, cobalamin, biotin, folic acid, I-inositol, niacinamide, D-calcium pantothenate, pyridoxine hydrochloride, riboflavin, and thiamine hydrochloride), five trace minerals (cupric sulfate, ferric sulfate, ferric nitrate, zinc sulfate, and sodium selenite), and growth factors, including basic fibroblast growth factor. Compared with StemFit medium, the quantities of most ingredients were increased for large-scale culture.

Alkaline phosphatase staining

Alkaline phosphatase staining was performed using a Leukocyte Alkaline Phosphatase kit (Sigma) as described previously (Tohyama et al., 2016).

Visualization of gas exchange in a multilayered CP under AGV

A 10-layered culture plate (TAITEC) was filled with 2 L PBS with 20 mg phenol red, and 50 mL/min 5% CO_2 per layer was actively ventilated. A photograph was taken every 10 min.

Measurement of gas exchange rate

In order to measure the gas exchange rate in the AVG system, 500 mL/min N_2 was actively ventilated using the MG-70M multi-gas incubator (TAITEC) through the 10-layered CP. In the NGV system, the 10-layer CP was placed under hypoxic conditions (1% O_2). A sensor tip (SP-PSt3-YAU-D5; PreSens, Germany) and optical fiber (POF-1MSA; PreSens, Germany) were placed in the fifth layer of the 10-layer CP. The oxygen concentration was measured using Fibox 3 (PreSens, Germany).

Immunocytochemistry

Cells were fixed with 4% paraformaldehyde for 20 min. Subsequently, cells were permeabilized with 0.1% Triton X-100 (Sigma) at room temperature for 5 min and then incubated with primary antibodies, i.e., 1:500 dilution of mouse anti-α-actinin (Sigma, A7811), 1:200 dilution of mouse anti-cardiac troponin T (Thermo Scientific, MS-295-p), 1:200 dilution of mouse anti-MLC2a (Synaptic System, Germany, 311011), 1:200 dilution of rabbit anti-MLC2v (ProteinTech, USA, 10906-1-AP), 1:200 dilution of rabbit anti-NANOG (ReproCELL, Japan, RCAB003P), 1:200 dilution of mouse anti-OCT4 (Santa Cruz Biotechnology, USA, sc-5279), 1:200 dilution of anti-TRA1-60 (Millipore, Germany, MAB4360), 1:200 dilution of mouse anti-TRA1-81 (Millipore, MAB4381), and 1:200 dilution of mouse anti-SSEA4 (Millipore, MAB4304), overnight at 4°C. Cells were then washed with PBS containing 0.1% Tween 20 three times prior to incubation with secondary antibodies (Alexa Fluor 488/594 anti-mouse IgG or IgM and Alexa Fluor 488/594 anti-rabbit IgG) for 1 h at room temperature. After nuclear staining with Hoechst 33342 (Thermo Scientific), stained cells were detected by fluorescence microscopy (Axio Observer; Carl Zeiss, Jena, Germany).

FACS analysis

hiPSCs or differentiated CMs were completely dissociated using 0.25% trypsin-ethylenediaminetetraacetic acid (EDTA) and then fixed with 4% paraformaldehyde for 20 min. Subsequently, cells were permeabilized with 0.1% Triton X-100 (Sigma) at room temperature for 5 min and incubated with primary antibodies, i.e., 1:200 dilution of mouse anti-OCT4 (Santa Cruz Biotechnology, sc-5279), 1:200 dilution of mouse anti-TRA1-60 (Millipore, MAB4360), 1:200 dilution of mouse anti-SSEA4 (Millipore, MAB4304), and 1:200 dilution of mouse anti-cardiac troponin T (Thermo Scientific, MS-295-p), at 4°C overnight. Cells were washed with PBS containing 0.1% Tween 20 prior to incubation with

Alexa 488 donkey anti-mouse IgG secondary antibodies (Thermo Scientific) at room temperature for 2 h. Cells were analyzed by FACS. Negative controls used for gating were based on the cells stained with isotype control antibodies.

Cryopreservation of purified hiPSC-CMs

After purification, the cells were isolated using 0.25% trypsin-EDTA for 10 min at 37°C. The isolated cells were counted using a ViCell (Beckman Coulter) and cryopreserved in STEM-CELLBANKER (Nippon Zenyaku Kogyo Co., Ltd., Japan) using BICELL (Nihon Freezer, Japan). After thawing the hiPSC (253G4 and FfI14)-CMs, cell viabilities were evaluated by trypan blue staining using a Vi-Cell cell counter (Beckman Coulter).

Action potential recordings

After thawing the hiPSC (253G4)-CMs, cells were seeded on fibronectin-coated (Sigma) probes. Then, action potentials were recorded as previously described (Hemmi et al., 2014; López-Redondo et al., 2016). Current-clamp recording was conducted in normal Tyrode's solution containing 135 mM NaCl, 0.33 mM NaH_2PO_4, 5.4 mM KCl, 1.8 mM $CaCl_2$, 0.53 mM $MgCl_2$, 5.5 mM glucose, and 5 mM HEPES (pH 7.4 at 35°C) using the pipette solution: 60 mM KOH, 80 mM KCL, 40 mM aspartate, 5 mM HEPES, 10 mM EGTA, 5 mM Mg ATP, 5 mM sodium creatinine phosphate, and 0.65 mM $CaCl_2$ (pH 7.2 adjusted with KOH). Amphotericin B was added to the pipette solution (final concentration 0.3 g/L) to perforate the cell membrane just before use.

Field potential recordings using a multi-electrode array system

To characterize the functional properties of our purified hiPSC (253G4)-derived CMs, we performed extracellular recording of field potentials (FPs) using a multi-electrode array

(MEA) system (MED 64; AlphaMED Scientific, Japan), as described previously (Egashira et al., 2012; Nakamura et al., 2014; Tanaka et al., 2009). After thawing of hiPSC-derived CMs, cells were seeded on fibronectin-coated (Sigma) probes. The recorded extracellular electrograms were used to determine field potential duration (FPD), defined as the time interval between the initial deflection of the FP and the maximum T wave. FPD measurements were corrected by Bazett's correction formulae (corrected FPD = FPD / [RR interval]$^{1/2}$), where RR indicates the time interval (s) between two consecutive beats. The temperature was maintained at 37°C during these recordings. After incubation for 10–15 min with E4031 (a gift from Esai, Japan) or (-)-isoproterenol hydrochloride (Sigma), the FPs were measured. In experiments using E4031, different channels were analyzed in the MEA probe. In experiments using isoproterenol, different probes were analyzed. The temperature was maintained at 37°C during these recordings.

Statistics

Values are presented as means ± SD or SEM. Statistical significance was evaluated using Student's t tests for comparisons between two mean values. Multiple comparisons between more than three groups were performed using analysis of variance with Dunnett's multiple comparison tests. Results with *p* values of less than 0.05 were considered significant.

References

Egashira, T., Yuasa, S., Suzuki, T., Aizawa, Y., Yamakawa, H., Matsuhashi, T., Ohno, Y., Tohyama, S., Okata, S., Seki, T.*, et al.* (2012). Disease characterization using LQTS-specific induced pluripotent stem cells. Cardiovasc Res *95*, 419-429.

Hemmi, N., Tohyama, S., Nakajima, K., Kanazawa, H., Suzuki, T., Hattori, F., Seki, T., Kishino, Y., Hirano, A., Okada, M.*, et al.* (2014). A Massive Suspension Culture System With Metabolic Purification for Human Pluripotent Stem Cell-Derived Cardiomyocytes. Stem Cells Translational Medicine *3*, 1473-1483.

Lian, X., Hsiao, C., Wilson, G., Zhu, K., Hazeltine, L.B., Azarin, S.M., Raval, K.K., Zhang, J., Kamp, T.J., and Palecek, S.P. (2012). Robust cardiomyocyte differentiation from human pluripotent stem cells via temporal modulation of canonical Wnt signaling. Proc Natl Acad Sci U S A *109*, E1848-1857.

López-Redondo, F., Kurokawa, J., Nomura, F., Kaneko, T., Hamada, T., Furukawa, T., and Yasuda, K. (2016). A distribution analysis of action potential parameters obtained from patch-clamped human stem cell-derived cardiomyocytes. Journal of Pharmacological Sciences *131*, 141-145.

Nakagawa, M., Taniguchi, Y., Senda, S., Takizawa, N., Ichisaka, T., Asano, K., Morizane, A., Doi, D., Takahashi, J., Nishizawa, M.*, et al.* (2014). A novel efficient feeder-free culture system for the derivation of human induced pluripotent stem cells. Sci Rep *4*, 3594.

Nakamura, Y., Matsuo, J., Miyamoto, N., Ojima, A., Ando, K., Kanda, Y., Sawada, K., Sugiyama, A., and Sekino, Y. (2014). Assessment of Testing Methods for Drug-Induced Repolarization Delay and Arrhythmias in an iPS Cell–Derived Cardiomyocyte Sheet: Multi-site Validation Study. Journal of Pharmacological Sciences *124*, 494-501.

Tanaka, T., Tohyama, S., Murata, M., Nomura, F., Kaneko, T., Chen, H., Hattori, F., Egashira, T., Seki, T., Ohno, Y.*, et al.* (2009). In vitro pharmacologic testing using human

induced pluripotent stem cell-derived cardiomyocytes. Biochem Biophys Res Commun *385*, 497-502.

Tohyama, S., Fujita, J., Hishiki, T., Matsuura, T., Hattori, F., Ohno, R., Kanazawa, H., Seki, T., Nakajima, K., Kishino, Y.*, et al.* (2016). Glutamine Oxidation Is Indispensable for Survival of Human Pluripotent Stem Cells. Cell Metab *23*, 663-674.